Reverse Large Well Method-Based Identification of Dewatering Parameters and Correction of Water Inflow for Deep Excavations in Highly Permeable Sandy Gravel Strata

Xiaotong Yan[1,*], Kang Sun[2], Shenwei Gao[3]
[1]School of Architectural Engineering,Shenyang University， Shenyang ,110041, Liaoning, China.
[2]Shenyang Dibo Construction Engineering Co., Ltd., Shenyang ,110031, Liaoning, China.
[3]Shenyang Dibo Construction Engineering Co., Ltd., Shenyang ,110031, Liaoning, China.
Corresponding author: Xiaotong Yan (Email: 15734010666@163.com)

ABSTRACT Deep excavation dewatering in highly permeable sandy gravel strata faces two major challenges: distorted parameter estimation and inaccurate prediction of water inflow. This study investigates four representative deep excavation projects in Shenyang --Zhonghai Huanyu Foundation Pit, Xinlipu Bridge Subway Station, Shenyang University Subway Station, and Chang'an Bridge South Subway Station. An intelligent dewatering monitoring system was introduced to obtain high-frequency groundwater level and flow rate data. A quasi-steady-state identification method based on a sliding time window was developed, and a segmented hydraulic conductivity inversion model was established using the reverse large well method. The results reveal significant vertical heterogeneity in the stratigraphy at all four sites, with hydraulic conductivity in the middle and lower layers generally higher than that in the upper layers. The overall weighted hydraulic conductivity values are 79.44, 115.01, 87.02, and 114.21 m/d, respectively. The hydraulic conductivity values suggested by site investigations were generally overestimated, with an average correction factor α_k of 0.9034, recommended as 0.90. Water inflow calculated by the conventional large well method was generally overestimated, with an average correction factor β_Q of 0.641, recommended as 0.65. A three-dimensional transient seepage model established using GMS-MODFLOW achieved coefficients of determination greater than 0.90 for simulating the water level variation processes at four observation wells. The inverted parameters and analytical calculations show high consistency in both magnitude and vertical variation patterns. The proposed technical framework--"field monitoring inversion→parameter correction→numerical validation"--provides a reliable methodological support and engineering reference for dewatering design in deep excavations within highly permeable sandy gravel strata.

INDEX TERMS Reverse large well method; deep excavation dewatering; highly permeable sandy gravel strata; parameter inversion; water inflow correction; numerical simulation

I. INTRODUCTION

The rapid development of urban rail transit has led to deep foundation pit engineering becoming increasingly deep, dense, and situated in complex environmental conditions. As a key technology for controlling construction safety and environmental impacts in underground engineering, the rationality of dewatering design directly affects foundation pit stability and the safety of surrounding structures [1]. In Shenyang, Quaternary alluvial-proluvial sand-gravel and rounded gravel strata with high permeability are widely distributed. These strata are characterized by coarse particles, well-developed pore channels, high permeability, and significant vertical heterogeneity. Under such site conditions, the dewatering process is influenced by multiple factors, including stratified hydraulic conductivity differences, recharge from nearby rivers, seepage around cutoff structures, and well interference, leading to a complex actual seepage field.

The conventional large-well method has been widely used in foundation pit dewatering design due to its simplicity and clear formulation [2]–[5]. However, its idealized assumptions have gradually revealed limitations in highly permeable sand-gravel strata. For example, the equal-area equivalent radius method for elongated foundation pits fails to adequately capture the long-side control effect. The radius of influence, often determined by empirical formulas, may deviate from actual recharge boundary conditions in high-permeability sites. Furthermore, well interference and non-Darcy effects under high hydraulic gradient conditions can lead to systematic discrepancies between theoretical calculations and field responses [6]. Existing research has primarily focused on modifications to the model form itself, such as equivalent radius adjustment, boundary condition optimization, and well group superposition methods [7], [8]. However, the issue of inadequate parameter representativeness has received relatively limited attention. In highly permeable sand-gravel strata, the deviation of the conventional large-well method likely stems from inconsistencies between geotechnical investigation parameters, stratified water supply characteristics, and actual conditions during the construction period.

In recent years, the application of intelligent dewatering monitoring systems has enabled continuous acquisition of high-frequency data at construction sites, including well group flow rates, water level changes, and equipment operation status [9], [10]. This provides a data foundation for parameter inversion based on monitoring constraints and enables the transformation of traditional analytical calculations from empirical estimation to dynamic calibration. Although progress has been made in parameter inversion studies [11]–[13], most research has aimed to obtain overall average parameters, with insufficient attention given to stratified permeability differences and their influence on water inflow evolution. The causes of differences between inverted parameters and investigation values, their engineering equivalence significance, and how they can be used to modify conventional design methods remain inadequately discussed.

Therefore, based on four typical deep foundation pit projects in Shenyang, this study established a reverse large-well method for the segmental inversion of permeability coefficients using high-frequency data from an intelligent dewatering monitoring system. Engineering correction factors for permeability coefficients and water inflow were proposed and validated through three-dimensional numerical simulation. This research aimed to address two core problems—inconsistency between geotechnical investigation parameters and actual construction responses, and deviation in water inflow predictions using the conventional large-well method—thereby providing a reliable methodological basis and parameter guidance for dewatering design in similar projects.

II. MATERIALS AND METHODS

A. ENGINEERING BACKGROUND AND HYDROGEOLOGICAL CONDITIONS

This study investigated four typical deep foundation pit projects in Shenyang: Xinlipuqiao Station, Zhonghai Huanyu Foundation Pit, Shenyang University Station, and Chang' anqiao South Station. The strata at each site are dominated by Quaternary alluvial-proluvial sand-gravel and rounded gravel layers, characterized by high permeability and significant vertical heterogeneity [14]–[17]. The basic characteristics of each site are summarized in Table 1.

TABLE 1. Basic Characteristics of the Four Typical Project Sites

Project site	Excavation depth/m	Major aquifer	Investigation permeability coefficient/ $m \cdot d^{-1}$	Hydrogeological characteristics
Xinlipuqiao Station	-18	rounded gravel⑤5、⑥5	130	Adjacent to Hun River; strong lateral recharge
Zhonghai Huanyu Foundation Pit	-15	gravelly sand、rounded gravel	95	Urban built-up area; environmentally sensitive
Shenyang University Station	-26	gravelly sand ④4、⑤4	85	Distant from river; limited recharge

Xinlipuqiao Station and Chang' anqiao South Station are located adjacent to the Hunhe River and are significantly influenced by lateral recharge from the river. The aquifer is dominated by rounded gravel with high permeability. Shenyang University Station is located away from the river, with relatively limited recharge conditions. Zhonghai Huanyu Foundation Pit is situated in a mature urban area with dense surroundings and high requirements for deformation control.

B. INTELLIGENT DEWATERING MONITORING SYSTEM

The intelligent dewatering monitoring system for foundation pits consists of four components: a sensor network, a data acquisition and communication unit, a cloud platform, and an intelligent analysis and early warning module. The system deploys water level sensors and flow meters in the foundation pit area, and the collected data are transmitted in real time to the cloud platform via IoT gateways, enabling real-time monitoring and control of water levels, flow rates, and pump power, as shown in Figure 1.

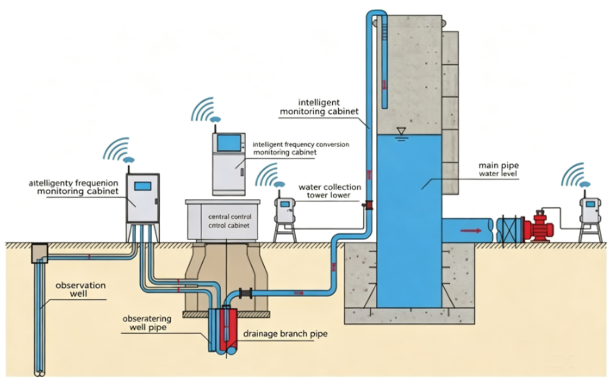

Fig. 1. Schematic Diagram of the Working Principle of the Intelligent Dewatering Monitoring System.

Compared with conventional manual monitoring, this system offers the following advantages: (1) real-time capability: second-level or minute-level data updates capture rapid dynamic changes in groundwater;
(2) accuracy: automated acquisition reduces human error and significantly improves data quality; (3) continuity: uninterrupted monitoring throughout the entire dewatering process, from startup to stabilization; (4) economy: intelligent

control of pump startup and shutdown based on actual demand, with optimization of operation schedules using peak-valley electricity pricing.

This study acquired high-frequency monitoring data throughout the dewatering processes at the four sites, including hourly flow rates from each dewatering well, water level changes in observation wells inside and outside the pits, and equipment operation status, providing a reliable data foundation for parameter inversion.

C. REVERSE LARGE-WELL METHOD FOR PARAMETER INVERSION

1) METHOD PRINCIPLES

The conventional large-well method simplifies discrete pumping wells in a foundation pit into a single equivalent large well, establishing the relationship between water inflow and drawdown based on Dupuit' s steady-state flow theory [18], [20]. For a fully penetrating unconfined well, the expression is:

$$Q = 1.366K\frac{2HS_W - S_W^2}{\lg R - \lg r_0} \tag{1}$$

where Q is the total water inflow into the pit (m^3/d), K is the permeability coefficient (m/d), H is the aquifer thickness (m), S_W is the design drawdown (m), R is the radius of influence (m), and r_0 is the equivalent radius of the foundation pit (m).

The conventional method is a forward prediction approach, and its results are highly dependent on the accuracy of input parameters. The reverse large-well method proposed in this study uses monitoring data as constraints, transforming the forward analytical process into a parameter inversion: the measured total water inflow Q and regional drawdown S are taken as known quantities, and the permeability coefficient K is solved inversely. The core of this method lies in dividing the aquifer into several segments along the depth direction and inverting the permeability coefficient of each segment step by step using data from quasi-steady-state stages.

2) QUASI-STEADY-STATE IDENTIFICATION AND SEGMENTATION METHOD

In the segmented inversion of formation permeability, the selection of the drawdown increment $\triangle h_i$ directly affects the identification of permeability differences between layers. This study did not preset $\triangle h_i$ empirically but instead adaptively determined segmentation nodes based on monitoring data. A moving time window was used to perform real-time statistics on the total well group flow rate series $Q_{(t)}$. The mean $Q_{(k)}$ and standard deviation $\sigma_{(Q,k)}$ of the data within each time window were calculated. A quasi-steady state was considered to be achieved when both flow stability and drawdown stability criteria were satisfied within a given time window [21].The flow stability criterion is:

$$\eta_{Q,k} = \frac{|\overline{Q_k} - \overline{Q_{k-1}}|}{\overline{Q_{k-1}}} \le \varepsilon_Q \tag{2}$$

where $\eta_{Q,k}$ is the relative change rate of the mean flow between adjacent time windows, $\overline{Q_k}$ is the mean flow within the k-th time window (m^3/d), $\overline{Q_{k-1}}$ is the mean flow within the (k-1)-th time window (m^3/d), and ε_Q is the threshold for the relative change rate of mean flow.

$$CV_{Q,k} = \frac{\sigma_{\alpha,k}}{\overline{Q_k}} \le C_{VQ} \tag{3}$$

where $CV_{Q,k}$ is the coefficient of variation of flow within the k-th time window, and C_{VQ} is the flow fluctuation threshold used to exclude unstable periods where the mean flow changes little but local fluctuations remain significant.

The drawdown stability criterion is:

$$\eta_{s,k} = \frac{|\overline{S_k} - \overline{S_{k-1}}|}{\max(\overline{S_{k-1}},0.5)} \le \varepsilon_S, \quad \Delta s_k \le s_0 \tag{4}$$

where $\overline{S_k}$ is the mean drawdown within the k-th time window (m), $\eta_{s,k}$ is the change rate of mean drawdown between adjacent windows,ε_S is the threshold for drawdown change rate, $\triangle s_k$ is the range of drawdown within the k-th time window (m), and s_0 is the upper limit of allowable minor fluctuations (m).

In this study, the moving time window $\triangle T$was set to 24h, the flow change rate threshold$\varepsilon_Q$was 0.05, the coefficient of variation threshold $C_{VQ}$was 0.10, the drawdown change rate threshold ε_S was 0.02, and the drawdown range upper limit s_0 was 0.10 m. The drawdown difference between the representative times of adjacent stable segments was defined as $\triangle h_i$, thus achieving adaptive determination of the segmentation.

3) SEGMENTAL PERMEABILITY COEFFICIENT INVERSION

For the i-th segment, using the corresponding drawdown increment $\triangle h_i$and the total pumping rate of the well group Q_i, the permeability coefficient K_i of that segment was inverted based on the steady-state flow model for a single well:

$$K_i' = \frac{Q_i}{\pi\left[H_0^2 - \left(H_0 - \sum_{i=1}^{m} \Delta H_i + S_w\right)^2\right]} \cdot \ln\frac{R_i}{r_w} \tag{5}$$

$$K_i = \frac{K_i' \cdot \sum_{i=1}^{m} \Delta h_i - \sum_{i=1}^{m} K_{i-1} \cdot \Delta h_{i-1}}{\Delta h_i} \tag{6}$$

where $K_i^{'}$ is the horizontal equivalent permeability coefficient of the formation within the drawdown range $\sum_{i=1}^{n} \Delta h_i$(m/d), Q_i is the water inflow into the pit during the drawdown process $\sum_{i=1}^{n} \Delta h_i$ (m^3/d), H_0 is the thickness of the unconfined aquifer before dewatering (m), $\sum_{i=1}^{n} \Delta h_i$

is the drawdown of the equivalent large well (m),S_w is the well loss of the equivalent large well (m), R_i is the radius of influence corresponding to drawdown $\sum_{i=1}^{n} \Delta h_i$(m), and r_w is the radius of the equivalent large well (m).

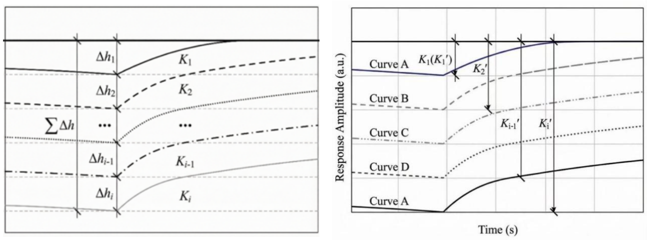

Fig. 2. Schematic Diagram of Stratigraphic Layering (Left) and Back-Calculation of the Permeability Coefficient of Soil Layers (Right).

The overall equivalent permeability coefficient$K_W$was obtained by thickness-weighted averaging:

$$K_w = \frac{\sum_{i=1}^{n} K_i \cdot \Delta h_i}{\sum_{i=1}^{n} \Delta h_i} \tag{7}$$

where$K_W$is the overall weighted permeability coefficient(m/d), $K_i$is the inverted permeability coefficient of the i-th segment (m/d), Δh_i is the thickness of the i-th segment (m), and n is the total number of segments.

D. THREE-DIMENSIONAL NUMERICAL SIMULATION

1) MODEL SETUP

A three-dimensional transient seepage numerical model was established based on GMS-MODFLOW [22] to independently validate the inverted parameters. The model covered a plan area of $177m \times 22m$, consistent with the study area. Vertically, the model was divided into five computational layers corresponding to the stratigraphic structure and aquifer characteristics.
(1) Boundary conditions: A general head boundary (GHB) was applied to the four sides of the model, with a reference head of 40.00 m (initial groundwater level), uniformly set across all five computational layers to represent lateral recharge from the external groundwater system [23], [24].
(2) Pumping conditions: A total of 42 dewatering wells were installed around the foundation pit. Pumping data were input based on field monitoring records, including total discharge and partial single-well pumping rates.
(3) Initial parameter assignment: Permeability and storage parameters for each layer were set according to stratigraphic characteristics and inversion results. Horizontal permeability coefficients K_h ranged from 52 to 102 m/d, and vertical permeability coefficients K_v were taken as 0.2 times K_h to reflect anisotropy.

2) MODEL CALIBRATION

Model calibration was performed using water level monitoring data from four observation wells (J1, J30, J37, J42) throughout the entire process. The simulation period spanned from October 29, 2024, to October 6, 2025, a total of 342 days. The fitting quality was evaluated using the root mean square error (RMSE), mean absolute error (MAE), and coefficient of determination (R^2).

III. RESULTS

A. SEGMENTAL PERMEABILITY COEFFICIENT INVERSION RESULTS

The segmental inversion results for the four sites are shown in Tables 2–5.

TABLE 2. Segmental Permeability Coefficient Inversion Results for Xinlipuqiao Station

Layer	Water Level Range /m	Thickness Δh_i(m)	Stage Inflow Q(m^3/d)	Inverted K_i(m/d)
$K1$	44.37–39.15	5.22	33680	95
$K2$	39.15–35.56	3.59	26170	120
$K3$	35.56–31.67	3.89	28710	135
$K4$	31.67–29.72	1.95	11630	119.5

TABLE 3. Segmental Permeability Coefficient Inversion Results for Zhonghai Huanyu Foundation Pit

Layer	Water Level Range /m	Thickness Δh_i(m)	Stage Inflow Q(m^3/d)	Inverted K_i(m/d)
$K1$	36.70–33.56	3.14	17025	67.5
$K2$	33.56–29.41	4.15	25450	85.19
$K3$	29.41–21.56	7.85	43820	95.8

TABLE 4. Segmental Permeability Coefficient Inversion Results for Shenyang University Station

Layer	Water Level Range /m	Thickness Δh_i(m)	Stage Inflow Q(m^3/d)	Inverted K_i(m/d)
$K1$	41.50–36.84	4.66	16330	55.02
$K2$	36.84–30.26	6.58	26930	75.01
$K3$	30.26–23.64	6.62	27560	95
$K4$	23.64–19.01	4.63	14140	88.04

TABLE 5. Segmental Permeability Coefficient Inversion Results for Chang'anqiao South Station

Layer	Water Level Range /m	Thickness Δh_i(m)	Stage Inflow Q(m^3/d)	Inverted K_i(m/d)
$K1$	43.86–40.11	3.75	8997.16	85.4
$K2$	40.11–35.47	4.64	13751.89	105.1
$K3$	35.47–30.26	5.21	19117.7	129.9
$K4$	30.26–25.16	5.1	18411.78	114.2

The inversion results for all four sites showed significant vertical heterogeneity in permeability, with permeability coefficients in the middle and lower layers generally higher than those in the upper layers. At Xinlipuqiao Station, the K3 layer reached 135 m/d; at Chang' anqiao South Station, the K3 layer reached 129.9 m/d, both serving as the main water-conducting layers. At Shenyang University Station, K increased from 55.02 m/d (K1) to 95.00 m/d (K3), and at Zhonghai Huanyu Foundation Pit, K increased from 67.50 m/d (K1) to 95.80 m/d (K3). These results indicate that it is unreasonable to simply treat highly permeable sand-gravel strata as a homogeneous aquifer.

B. OVERALL WEIGHTED PERMEABILITY COEFFICIENT AND CORRECTION

The calculated overall weighted permeability coefficients Kw are presented in Table 6.

TABLE 6. Overall Weighted Permeability Coefficients and Correction Factors at Each Site

Site	Investigation K_c/m·d^{-1}	Inverted K_w/m·d^{-1}	Inverted α_k	Site
Xinlipuqiao Station	130	115.01	0.8847	Xinlipuqiao Station
Zhonghai Huanyu Pit	95	87.02	0.9159	Zhonghai Huanyu Pit
Shenyang University Station	85	79.44	0.9346	Shenyang University Station
Chang'anqiao South Station	130	114.21	0.8785	Chang'anqiao South Station

The correction factors α_k at the four sites are all less than 1, with an average value of 0.9034, indicating that the recommended permeability coefficients from geotechnical investigations are generally overestimated. Considering the convenience of engineering application, a recommended correction factor of 0.90 is suggested for similar highly permeable sand-gravel strata in Shenyang, i.e.,$K^{‘} = 0.90K_c$

C. WATER INFLOW CORRECTION MODEL

A comparison between the theoretical water inflow calculated by the conventional large-well method and the measured stable water inflow in the field is shown in Table 7.

TABLE 7. Water Inflow Calculation Results and Correction Factors at Each Site

Site	Theoretical Inflow Q_t/m^3·d^{-1}	Measured Inflow Q_a/m^3·d^{-1}	Correction Factor β_Q
Xinlipuqiao Station	69981	43201	0.6173
Zhonghai Huanyu Pit	45870	30888	0.6734
Shenyang University Station	58545	38459	0.6569
Chang'anqiao South Station	64288	41528	0.6406

The correction factors β_Q at all sites are less than 1, ranging from 0.6173 to 0.6734, with an average value of 0.641. Considering the convenience of engineering application, a recommended water inflow correction factor of 0.65 is suggested, i.e.,$Q = 0.65Q_t$. This corrected value can be used for pre-construction dewatering design to guide well group layout and pump selection, while the theoretical value should still be used for safety checks of key components, balancing economy and safety.

D. Q-T CURVE EVOLUTION CHARACTERISTICS

The Q-T curves of the dewatering processes at the four sites exhibited different evolution patterns (Figure 3), reflecting the differences in boundary recharge conditions and stratigraphic permeability structures.

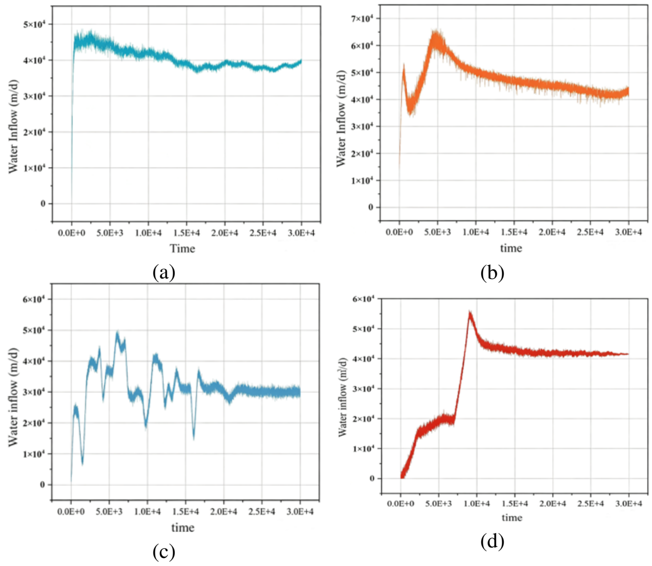

Fig. 3. Q-T Curves of the Four Sites: (a) Shenyang University Station; (b) Xinlipuqiao Station; (c) Zhonghai Huanyu Foundation Pit; (d) Chang'anqiao South Station.

(1) Shenyang University Station: The curve was relatively flat overall, with a significant and long-lasting plateau. In the early stage of dewatering, the inflow rapidly rose to approximately 4.0 × 10^4 m^3/d and then stabilized between 3.5×10^4 and 3.8 × 10^4 m^3/d. This indicated relatively low permeability (55–95 m/d) and limited lateral recharge at this site, with inflow mainly sustained by the release of stored water within the pit and limited lateral recharge.

(2) Xinlipuqiao Station: The curve exhibited a "hump" shape characterized by an initial rise, followed by a slow decline, and eventual stabilization. The initial inflow was approximately 3.5×10^4 m^3/d, rising to a peak of approximately 6.2×10^4 m^3/d at T ≈ 8000, then slowly declining to a stable value of 4.0×10^4 m^3/d. This reflected the strong lateral recharge in the high-permeability site adjacent to the river: during early dewatering, large-scale lateral recharge was activated; as the hydraulic gradient decreased, the inflow slowly declined but remained at a relatively high level.

(3) Zhonghai Huanyu Foundation Pit: The curve exhibited significant multi-peak oscillatory characteristics. The inflow rapidly rose to 3.0×10^4 m^3/d in the early stage, then declined. During the middle stage, it rose twice to 4.5×10^4 m^3/d, and finally stabilized at approximately 3.0×10^4 m^3/d. This reflected that different layers contributed to the water supply sequentially during the dewatering process: after the shallow layer was rapidly depleted, the middle–deep high-permeability layers were gradually activated, and the inflow declined when the available water in these layers was exhausted.

(4) Chang' anqiao South Station: The curve showed an initial increase, followed by a mid-stage rise, and then a high-level stabilization. The inflow rose to 2.0×10^4 m^3/d in the early stage, reached a peak of approximately 5.5×10^4 m^3/d at T≈ 9000, and then stabilized at approximately

4.2×10^4 m^3/d. This reflected the combined effect of initial stored water release and strong external recharge.

The Q-T curves not only reflected the influences of stored water release, external recharge, and stratified water supply but could also be used to characterize site hydrogeological conditions and identify dewatering stabilization stages, providing an important basis for parameter inversion.

E. NUMERICAL SIMULATION RESULTS

1) MODEL CALIBRATION

The fitting results (Figures 4–7) showed that the model successfully reproduced the overall water level variation processes at the four observation wells, capturing the characteristic stages of rapid initial decline, slow mid-term adjustment, and gradual late-term stabilization.

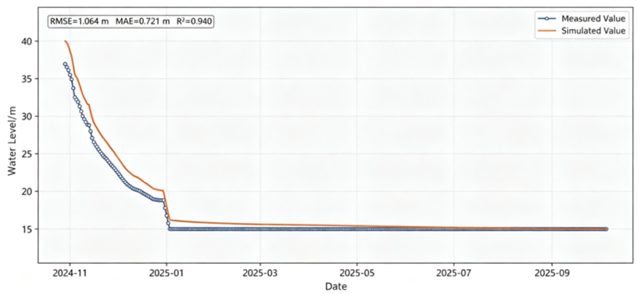

Fig. 4. Fitting Curve for Observation Well J1.

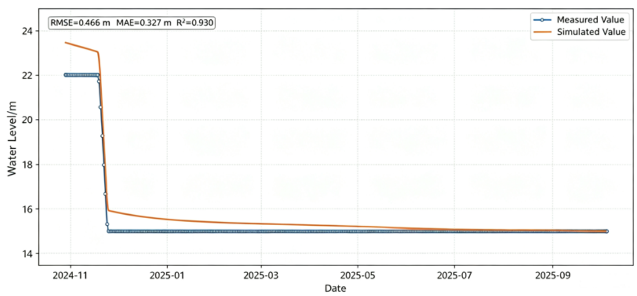

Fig. 5. Fitting Curve for Observation Well J30.

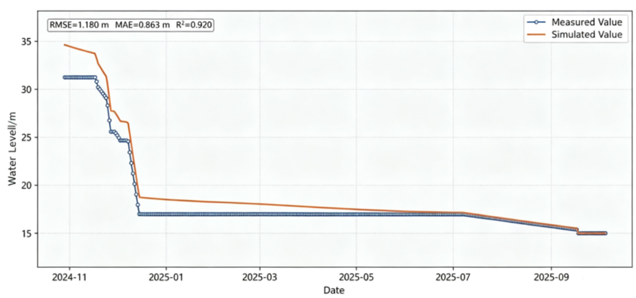

Fig. 6. Fitting Curve for Observation Well J37.

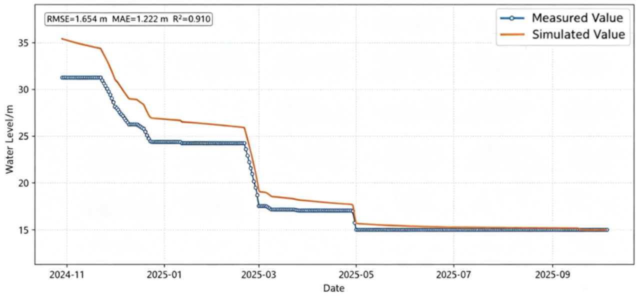

Fig. 7. Fitting Curve for Observation Well J42.

The fitting error statistics for each observation well are presented in Table 8.

TABLE 8. Fitting Error Statistics for Observation Wells

Observation Well	RMSE/m	MAE/m	R^2
J1	1.064	0.721	0.94
J30	0.466	0.327	0.93
J37	1.18	0.863	0.92
J42	1.654	1.222	0.91

The coefficient of determination $R^2$for each observation well exceeded 0.90, and the RMSE values were within 2 m, indicating high fitting accuracy. J30 showed the smallest errors, while J42 exhibited relatively larger errors, but its R^2remained high, suggesting that the deviations were mainly local amplitude differences rather than overall trend mismatches.

2) VERTICAL RESPONSE AND FLOW FIELD EVOLUTION

The variation in average water level across different layers (Figure 8) showed that the groundwater system in the study area exhibited significant vertically differentiated response characteristics. The upper layers responded first to pumping, with relatively rapid water level declines; the middle and lower layers showed a delayed response, indicating that pumping disturbances propagated downward through interlayer hydraulic connections. As pumping continued, water levels in all layers gradually converged to lower levels, and the system transitioned from layered response to overall reorganization.

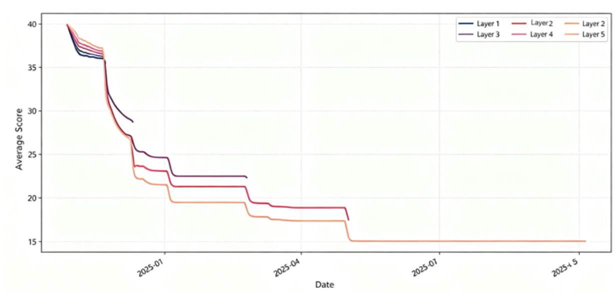

Fig. 8. Variation in Average Water Level at Different Layers.

Flow field evolution at typical times (Figure 9) indicated that at the early stage (4.2 d), pumping influence was limited to the vicinity of the well group; at the middle stage (29.2–119.2d), the low-water-level zone gradually expanded, and the flow field transitioned to a pumping-controlled state; at the late stage (341.2 d), the flow field tended toward dynamic equilibrium, consistent with the stage-wise variation patterns reflected in the observation well fitting curves.

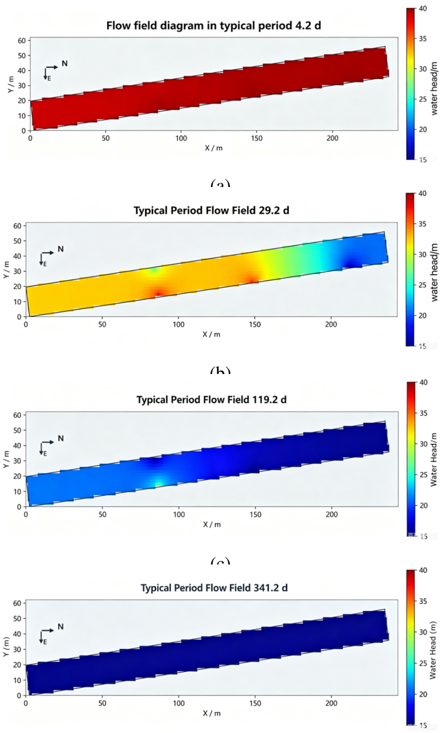

(d)

Fig. 9. Flow Field Evolution at Typical Times: (a) 4.2 d; (b) 29.2 d; (c) 119.2 d; (d) 341.2 d.

3) PARAMETER COMPARISON ANALYSIS

A comparison between the parameters inverted by numerical simulation and those obtained by analytical calculation is shown in Table 9.

TABLE 9. Comparison of Parameters from Analytical Calculation and Numerical Simulation

Layer	Analytical K/m·d^{-1}	Numerical K_h Range /m·d^{-1}	Numerical Mean K_h/m·d^{-1}	Analytical Value Falls Within Range
Layer1	55.02	52∼58	55	Yes
Layer2	75.01	70∼80	75	Yes
Layer3	95	88∼102	95	Yes
Layer4	88.04	82∼94	88	Yes

The analytical results for the first four layers all fell within the numerical simulation parameter ranges, demonstrating high consistency between the two methods in terms of magnitude and interlayer variation patterns. Numerical simulation further revealed intra-layer spatial heterogeneity through layered zoning parameters (three zones per layer), providing a more detailed representation of heterogeneity.

IV. DISCUSSION

A. CAUSES OF DEVIATION IN GEOTECHNICAL INVESTIGATION PARAMETERS

The permeability coefficient correction factors α_k at the four sites ranged from 0.8785 to 0.9346 (average 0.9034), indicating that the recommended values from geotechnical investigations were systematically overestimated by approximately 10%. This deviation arose from the following factors:

(1) Scale effect [25]: The radius of influence of pumping tests during the investigation phase is limited (typically several tens of meters), whereas foundation pit dewatering involves a range of several hundred meters. When high-permeability interlayers exist, small-scale tests cannot fully capture their contribution to hydraulic conductivity, but large-scale dewatering can activate these high-permeability pathways. This study found that high-permeability layers (K = 95–135 m/d) are commonly present in the middle and lower parts of the sand-gravel strata in Shenyang, and their contribution to overall hydraulic conductivity is fully realized during the construction period. However, investigation parameters cannot fully capture this characteristic.

(2) Stratified water supply characteristics [26]: Investigation parameters are mostly obtained from single pumping tests, reflecting the overall hydraulic conductivity of the aquifer. In contrast, construction dewatering requires progressive drainage of different layers, with distinct contributions from different layers to water supply. In this study, the deep high-permeability layers contributed over 60% of the total water inflow, serving as the dominant factor controlling total water inflow.

(3) Boundary recharge conditions: The near-river sites (Xinlipuqiao Station and Chang' anqiao South Station) are subject to constant-head recharge from the river. Investigation tests struggle to simulate this continuous recharge condition, leading to parameter overestimation.

B. MECHANISMS OF WATER INFLOW DEVIATION

The water inflow correction factors β_Q ranged from 0.6173 to 0.6734 (average 0.641). The sources of deviation included:

(1) Geometric generalization error [6]: The aspect ratio of subway station foundation pits can reach 10:1. The equal-area equivalent radius method ($r_0 = \sqrt{\frac{ab}{\pi}}$) simplifies the elongated pit into a circle, underestimating hydraulic losses along the long side. In elongated foundation pits, groundwater flow is characterized by bidirectional flow perpendicular to the long side rather than radial convergence toward the center. This leads to a smaller denominator in the logarithmic term, resulting in an overestimation of water inflow.

(2) Well interference effect [27]: The conventional large-well method assumes that the total water inflow of the well group equals the sum of individual well inflows, neglecting the reduction in individual well capacity due to interference. The interference effect is more significant in

highly permeable strata, resulting in actual total inflow lower than the theoretical superposition value.
(3) Recharge condition limitation: The radius of influence R determined by the empirical formula ($R = 2S\sqrt{KH}$) is overestimated for highly permeable near-river sites. In reality, the drawdown cone expansion is limited by the river boundary, leading to overestimation of theoretical water inflow.

C. ENGINEERING APPLICATION RECOMMENDATIONS

Based on the findings of this study, the following recommendations are proposed for engineering applications:
(1) Parameter value: For dewatering design in highly permeable sand-gravel and rounded gravel strata in Shenyang, it is recommended to first take 0.90 times the investigation-recommended permeability coefficient as an initial value, and then make minor adjustments based on site conditions and engineering experience.
(2) Water inflow prediction: Before construction, the theoretical water inflow calculated by the conventional large-well method can be multiplied by 0.65 for correction, which can be used for well layout design and pump selection. For safety checks of key components, the theoretical value should still be used.
(3) Dynamic control: It is recommended to use an intelligent dewatering monitoring system to track water inflow and water level changes in real time, identify dewatering stages based on Q-T curve morphology, and perform dynamic parameter correction when necessary.

D. APPLICABILITY AND LIMITATIONS OF THE METHOD

The method presented in this paper is applicable under the following conditions: (1) foundation pit engineering in highly permeable sand-gravel and rounded gravel strata; (2) use of a well group dewatering scheme; (3) availability of intelligent dewatering monitoring conditions.

Limitations include: (1) The correction factors are based on statistics from four sites in Shenyang and require validation with local conditions when applied to other regions; (2) The blocking effect of cutoff walls on seepage is not considered; appropriate corrections should be introduced when cutoff walls are present; (3) The influence of non-Darcy flow may be more significant under extremely high-velocity flow conditions and requires further investigation.

V. CONCLUSIONS

(1) This study established a reverse large-well method analytical framework based on monitoring constraints, transforming the conventional analytical method from forward prediction to parameter inversion. The quasi-steady-state identification method using a moving time window achieved adaptive determination of drawdown segmentation, overcoming the arbitrariness of empirical segmentation.
(2) The inversion results at the four sites showed significant vertical heterogeneity in the sand-gravel strata in Shenyang, with middle and lower high-permeability layers dominating the total water inflow. The overall weighted permeability coefficients were 79.44, 115.01, 87.02, and 114.21 m/d, respectively, indicating that a single average parameter from the investigation stage cannot accurately reflect the actual seepage characteristics.
(3) The average correction factor for permeability coefficients α_k was 0.9034, with a recommended value of 0.90; the average correction factor for water inflow β_Q was 0.641, with a recommended value of 0.65. Both correction factors exhibited stable statistical patterns and can guide the design of similar projects.
(4) The Q-T curves exhibited four evolution patterns: the limited-recharge gentle type (Shenyang University Station), the near-river strong-recharge "hump" type (Xinlipuqiao Station), the stratified-water-supply multi-peak oscillatory type (Zhonghai Huanyu Foundation Pit), and the mixed-recharge increase-stabilization type (Chang' anqiao South Station). These patterns can be used to distinguish site boundary conditions and identify dominant water-supply layers.
(5) Three-dimensional numerical simulation validation showed that the model achieved R^2 values greater than 0.90 for water level fitting at four observation wells. The inverted parameters were highly consistent with analytical results in magnitude and interlayer variation patterns, confirming the reliability of the parameter identification results. The proposed technical pathway of "field monitoring inversion→parameter correction→numerical validation" provides a reliable foundation for dewatering design in deep foundation pits in highly permeable sand-gravel strata.

AUTHOR CONTRIBUTIONS

Conceptualization, methodology, validation, X.H.; formal analysis, X.H.; investigation, X.H.; resources, X.H.; data curation, H.J.; writing—original draft preparation, H.J.; writing—review and editing, X.H.; visualization, H.J.; supervision, project administration, X.H., H.W., Y.S. All authors have read and agreed to the published version of the manuscript.

FUNDING

This research received no external funding

DATA AVAILABILITY STATEMENT

The data presented in this study are available on request from the corresponding author.

CONFLICTS OF INTEREST

The authors declare no conflicts of interest.

REFERENCES

[1] F. W. Wang, S. W. Liang, and A. J. Feng, “Data statistics and development analysis of urban rail transit in China in 2025,” Tunn. Constr., vol. 46, no. 02, pp. 437–444, 2026.
[2] T. Li, H. Song, G. Huang, et al., “Assessment of groundwater changing trends through the generalized large well method with confined-unconfined flow model in open-pit mine area,” Environmental Earth Sciences., vol. 72, no. 11, pp. 4599–4606, 2014.

[3] K. Yang, C. Xu, M. Chi, et al., "Analytical analysis of the groundwater drawdown difference induced by foundation pit dewatering with a suspended waterproof curtain," Applied Sciences., vol. 12, no. 20, p. 10301, 2022.
[4] Y. X. Sun, S. Y. Liu, L. Y. Tong, et al., "Optimization of confined aquifer dewatering for open-cut tunnel foundation pit in Yangtze River floodplain area," Rock Soil Mech., vol. 44, no. 06, pp. 1800–1810, 2023.
[5] Y. L. Mu, L. Kang, X. F. Yang, et al., "Calculation of water inflow into foundation pit in confined aquifer considering waterproof curtain," Ground Improv., vol. 6, no. 03, pp. 235–241, 2024.
[6] Z. P. Shi, "Well array method for dewatering calculation of rectangular foundation pits," Geotech. Investig. Surv., vol. 44, no. 11, pp. 31–36, 2016.
[7] JGJ 120-2012. Technical Specification for Retaining and Protection of Building Foundation Excavations. Beijing, China: China Architecture & Building Press, 2012.
[8] Z. X. Zhang and W. X. Li, "Comparative study of prediction methods for mine water inflow: A case study of Dazhuang Coal Mine in Gansu Province," Northwestern Geol., vol. 55, no. 03, pp. 355–360, 2022.
[9] J. Zhou, H. Xiao, W. Jiang, et al., "Automatic subway tunnel displacement monitoring using robotic total station," Measurement, vol. 151, p. 107251, 2020.
[10] X. Wang, M. Wang, R. Jiang, et al., "Structural deformation monitoring during tunnel construction: A review," J. Civ. Struct. Health Monit., vol. 14, no. 3, pp. 591–613, 2024.
[11] J. Chen and Z. Dai, "Metaheuristic algorithms for groundwater model parameter inversion: Advances and prospects," Deep Resour. Eng., vol. 1, no. 2, p. 100009, 2024.
[12] R. Ye, H. G. Di, Z. T. Zhu, et al., "Research on hydrogeological parameter inversion of confined aquifer in subway foundation pit based on surrogate model," Urban Mass Transit Res., vol. 28, no. 07, pp. 80–85+92, 2025.
[13] N. W. Liu, C. X. Peng, M. G. Li, et al., "Hydro-mechanical behavior of a deep excavation with dewatering and recharge in soft deposits," Eng. Geol., vol. 307, p. 106780, 2022.
[14] Geotechnical Investigation Report for Xinlipuqiao Station of Shenyang Metro Line 9. Shenyang, China, 2022.
[15] Geotechnical Investigation Report for Zone J of Zhonghai Huanyu Project. Shenyang, China, 2021.
[16] Geotechnical Investigation Report for Shenyang University Station. Shenyang, China, 2022.
[17] Geotechnical Investigation Report for Chang' anqiao South Station of Shenyang Metro Line 9. Shenyang, China, 2022.
[18] Z. F. Zhou and J. G. Wang, Groundwater Dynamics. Beijing, China: China Water & Power Press, 2021, p. 244.
[19] C. X. Chen, Z. H. Tang, Y. H. Xie, et al., "Island unconfined well flow model in layered heterogeneous aquifers with infiltration recharge," Bull. Geol. Sci. Technol., vol. 42, no. 04, pp. 15–26, 2023.
[20] X. S. Wang, Y. H. Xie, and C. X. Chen, "Two-dimensional profile numerical simulation method for steady flow in unconfined wells," Bull. Geol. Sci. Technol., vol. 42, no. 04, pp. 27–36, 2023.
[21] G. E. P. Box, G. M. Jenkins, G. C. Reinsel, et al., Time Series Analysis: Forecasting and Control, 5th ed.. Hoboken, NJ, USA: John Wiley & Sons, 2015.
[22] M. G. Mcdonald and A. W. Harbaugh, A Modular Three-Dimensional Finite-Difference Ground-Water Flow Model. Reston, VA, USA: US Geological Survey, 1988.
[23] Z. J. Luo, L. Li, T. Q. Yao, et al., "Coupled model of three-dimensional seepage and land subsidence for dewatering in deep foundation pits in loose confined aquifer areas," Chin. J. Geotech. Eng., vol. 28, no. 11, pp. 1947–1951, 2006.
[24] J. X. Zhang, "Numerical simulation analysis of foundation pit dewatering," Shanxi Archit., vol. 47, no. 04, pp. 61–63, 2021.
[25] R. P. Chapuis, "Predicting the saturated hydraulic conductivity of soils: A review," Bull. Eng. Geol. Environ., vol. 71, no. 3, pp. 401–434, 2012.
[26] C. H. Zhu, J. M. Liu, and Z. H. Wang, "Study on the influence of particle size distribution on the permeability coefficient of coarse-grained soils," Yellow River, no. 12, pp. 79–81, 2005.
[27] M. Almasoodi, T. Andrews, C. Johnston, et al., "A new method for interpreting well-to-well interference tests and quantifying the magnitude of production impact: Theory and applications in a multi-basin case study," Geomech. Geophys. Geo-Energy Geo-Resour., vol. 9, no. 1, p. 95, 2023.